

Heriot-Watt University

Heriot-Watt University
Research Gateway

Generation of orbital angular momentum bell states and their verification via accessible nonlinear witnesses

Agnew, Megan; Salvail, Jeff Z.; Leach, Jonathan; Boyd, Robert W

Published in:
Physical Review Letters

DOI:
[10.1103/PhysRevLett.111.030402](https://doi.org/10.1103/PhysRevLett.111.030402)

Publication date:
2013

[Link to publication in Heriot-Watt Research Gateway](#)

Citation for published version (APA):
Agnew, M., Salvail, J. Z., Leach, J., & Boyd, R. W. (2013). Generation of orbital angular momentum bell states and their verification via accessible nonlinear witnesses. *Physical Review Letters*, 111(3), [030402].
[10.1103/PhysRevLett.111.030402](https://doi.org/10.1103/PhysRevLett.111.030402)





Generation of Orbital Angular Momentum Bell States and Their Verification via Accessible Nonlinear Witnesses

Megan Agnew,¹ Jeff Z. Salvail,¹ Jonathan Leach,^{1,2} and Robert W. Boyd^{1,3}

¹*Department of Physics, University of Ottawa, 150 Louis Pasteur, Ottawa, Ontario, K1N 6N5 Canada*

²*IPaQS, SUPA, Heriot-Watt University, Edinburgh, EH14 4AS United Kingdom*

³*Institute of Optics, University of Rochester, Rochester, New York 14627, USA*

(Received 20 March 2013; published 15 July 2013)

The controlled generation of entangled states and their subsequent detection are integral aspects of quantum information science. In this Letter, we implement a simple and precise technique that produces any of the four Bell states in the orbital angular momentum degree of freedom. We then use these states to perform the first experimental demonstration of an accessible nonlinear entanglement witness. Such a witness determines entanglement by using the same measurements as required for a linear witness but can detect, in this case, twice as many states as a single linear witness can. We anticipate that our method of state preparation and nonlinear witnesses will have further uses in areas of quantum science, such as superdense coding and quantum key distribution.

DOI: [10.1103/PhysRevLett.111.030402](https://doi.org/10.1103/PhysRevLett.111.030402)

PACS numbers: 03.65.Ud, 03.67.Mn, 42.50.Ex, 42.50.Tx

The generation and controlled manipulation of quantum states is vital to existing and emerging quantum technologies. In particular, controlled unitary operations on entangled quantum states [1] play an essential role in many quantum information protocols. For example, superdense coding relies upon unitary operations as a means by which to encode information [2,3]. As a result, it is important to be able to accurately implement controlled unitary operations in quantum systems. Unitary operations are easily accomplished in the polarization degree of freedom by using half- and quarter-wave plates, and thus a range of entangled states can be obtained. In contrast, controlled unitary operations had not been previously implemented in the orbital angular momentum (OAM) degree of freedom to produce the same range of entangled states. Such operations are becoming increasingly important due to the emergence of OAM as a resource for quantum information science [4–9].

In addition to the manipulation of entangled states, the efficient detection of entanglement is also vital to quantum information applications [10]. An entanglement witness establishes directly whether a quantum state belonging to a certain class is entangled [11–16]. Linear entanglement witnesses [17–19], which are witnesses that depend linearly on expectation values, are efficient, as they require the fewest possible number of measurements that will give sufficient information about the state; however, in order to function optimally, they require prior knowledge of the form of the entangled state.

Alternatively, nonlinear entanglement witnesses improve upon an existing linear entanglement witness with a term that relies nonlinearly on expectation value [20–26]; thus, a nonlinear witness is able to verify entanglement over a significantly larger set of states compared to its linear counterpart. Considering the example of the Bell

states, one can construct a single nonlinear witness that will detect both correlated Bell states $|\Phi^+\rangle$ and $|\Phi^-\rangle$ and a single nonlinear witness that will detect both anticorrelated Bell states $|\Psi^+\rangle$ and $|\Psi^-\rangle$, something not possible by using linear witnesses. Importantly, a new class of nonlinear witness, called accessible nonlinear witnesses, enables the detection of this wider class of states using the same measurements as the linear witness [27].

The main result of our Letter is the controlled generation of a wide range of states entangled in their OAM and the subsequent verification of the entanglement of these states via accessible nonlinear entanglement witnesses. Our method is simple, precise, and the first implementation of such a procedure for OAM, and, importantly, the states generated include all the Bell states. We compare the expectation values of the nonlinear witnesses to those of the standard linear witnesses and establish that the nonlinear witnesses are capable of detecting entanglement over a wider range of states. The particular degree of freedom we choose to investigate is orbital angular momentum; however, our results are general in that the nonlinear witness procedures can be applied to other degrees of freedom such as polarization or spin.

Quantum state preparation.—We generate OAM entanglement [4,7,28] by using parametric down-conversion and perform unitary operations using Dove prisms. By changing the number of prisms in the system, we are able to choose between a correlated and an anticorrelated state. By changing the angle of the prisms, we are able to manipulate the phase between the entangled modes; see Fig. 1.

Light with orbital angular momentum $\ell\hbar$ is represented by the state $|\ell\rangle$ and has a helical phase front that depends on the value of ℓ . A Dove prism placed at an angle $\theta/2$ in the path of such light performs two actions on the transmitted light: first, the transverse cross section of any

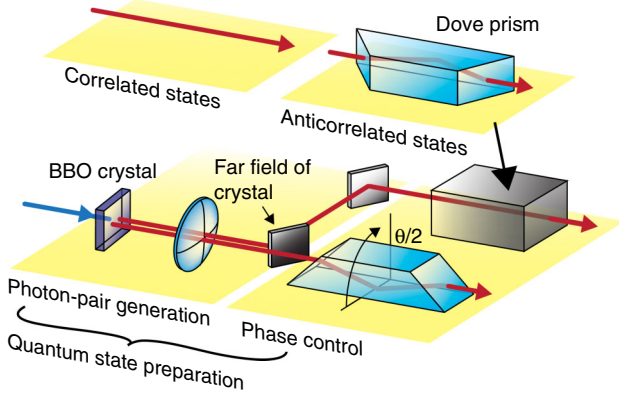


FIG. 1 (color online). Experimental setup. In the quantum state preparation stage, entangled photon pairs are generated by parametric down-conversion and are separated into two paths by a mirror. If a Dove prism is introduced into the upper path, anticorrelated states are produced. If no prism is placed in the upper path, correlated states are produced. The angle of the prism in the lower path controls the relative phase of the two modes.

transmitted beam is reversed such that $\ell \rightarrow -\ell$; second, an ℓ -dependent phase shift is introduced such that the modes within the beam acquire the additional phase $\ell\theta$. It follows that two Dove prisms can be used to introduce an ℓ -dependent phase shift between different OAM modes while leaving the sign of ℓ unchanged.

Light produced by parametric down-conversion is entangled in the orbital angular momentum basis as

$$|\Psi\rangle = \sum_{\ell=-\infty}^{\infty} c_{\ell} |\ell\rangle_A \otimes |-\ell\rangle_B, \quad (1)$$

where $|c_{\ell}|^2$ represents the probability that the photon in arm A has OAM $\ell\hbar$ and the photon in arm B has OAM $-\ell\hbar$. Placing a Dove prism in arm B of the down-conversion system, we obtain a correlated entangled state; i.e., the photons are both in the same state. Of particular interest are the two-dimensional subspaces that include the $|\ell = 0\rangle$ mode, as these are correlated entangled states of the form

$$|\Phi_{\ell}\rangle = \frac{1}{\sqrt{1 + \varepsilon_{\ell}^2}} (|0, 0\rangle + \varepsilon_{\ell} e^{i\varphi} |\ell, \ell\rangle), \quad (2)$$

where the phase $\varphi = \ell\theta_B$ is determined by the angle of the Dove prism $\theta_B/2$. Here we use $|a, b\rangle$ to be equivalent to $|a\rangle_A \otimes |b\rangle_B$. Placing a second Dove prism oriented at an angle $\theta_A/2$ in arm A of the system converts the state $|\Phi_{\ell}\rangle$ to an anticorrelated state

$$|\Psi_{\ell}\rangle = \frac{1}{\sqrt{1 + \varepsilon_{\ell}^2}} (|0, 0\rangle + \varepsilon_{\ell} e^{i\phi} |-\ell, \ell\rangle), \quad (3)$$

where $\phi = \ell(\theta_B - \theta_A)$. Using the states $|\Phi_{\ell}\rangle$ and $|\Psi_{\ell}\rangle$, we can test the ability of the nonlinear witness for detecting

entanglement of a large range of different states. The Bell states are particular cases of these states where $\varepsilon_{\ell} = 1$ and $\phi = 0, \pi$ or $\varphi = 0, \pi$. To our knowledge, this method has not been previously demonstrated and represents a new technique for quantum state preparation.

Entanglement witnesses.—The form of a mixed state containing an entangled state $|\psi\rangle$ is given by

$$\rho^{\psi} = |\psi\rangle\langle\psi|p + \mathbb{1}(1-p)/4, \quad (4)$$

where p is the probability of obtaining the entangled state $|\psi\rangle$ and $\mathbb{1}$ is the identity matrix, which represents uncolored noise. We use the superscript ψ to indicate that the convex combination ρ is partially composed of the entangled state $|\psi\rangle$. Whether or not the state ρ^{ψ} is entangled is determined by the probability p : States with $p > 1/3$ are entangled [10].

The expectation value w of an entanglement witness W on the quantum state ρ^{ψ} provides information about the state: A negative expectation value indicates entanglement, whereas a positive expectation value gives an inconclusive result. If a positive expectation value is obtained, the information gained is that either the state is separable or the witness chosen was not appropriate for the form of the entangled state.

One limitation of linear witnesses is that they function only over restricted sets of states: Entanglement of the set of states ρ^{Φ} (or ρ^{Ψ}) cannot be verified with a single linear witness. Recently, it was shown that it is possible to improve a linear witness with a term that relies nonlinearly on the expectation value [25,27,29]. One improvement is that entanglement of a significantly larger fraction of the set of states ρ^{Φ} (or ρ^{Ψ}) can be verified with a single nonlinear witness that contains the same observables as the linear witness. As an example, the entanglement of both the Bell states $|\Phi^{-}\rangle$ and $|\Phi^{+}\rangle$ can be confirmed by using a single nonlinear witness.

In our experiment, we compare the accessible nonlinear witnesses $W_{\infty}^{\Phi^{+}}$ and $W_{\infty}^{\Psi^{+}}$, where the ∞ subscript refers to the final iteration of the procedure for generating the witness [27,29], to their corresponding linear witnesses $W_L^{\Phi^{\pm}}$ and $W_L^{\Psi^{\pm}}$. The expectation value $w_{\infty}^{\Phi^{+}}$ of the witness $W_{\infty}^{\Phi^{+}}$ can be expressed as a combination of expectation values of measurable operators. Contained within the measurements for the nonlinear witness is a unitary operator U , which provides some freedom in choosing the exact form of the witness. By choosing U to be equal to $-\sigma_z \otimes \sigma_z$, we show in the Supplemental Material [30] that the expectation value of the particular nonlinear witness that we consider in this experiment is given by

$$w_{\infty}^{\Phi^{+}}(\rho) = \text{Tr}(\rho W_L^{\Phi^{+}}) - |\text{Tr}(\rho W_L^{\Phi^{+}})|^2 - \frac{|\text{Tr}(\rho W_L^{\Phi^{+}}) - \text{Tr}(\rho W_L^{\Phi^{+}}) \text{Tr}[\rho(-\sigma_z \otimes \sigma_z)]|^2}{1 - |\text{Tr}[\rho(-\sigma_z \otimes \sigma_z)]|^2}. \quad (5)$$

We see that $\text{Tr}(\rho W_L^{\Phi^+})$ and $\text{Tr}[\rho(-\sigma_z \otimes \sigma_z)]$ are the only measurements that are required for the nonlinear witness. A similar method may be used to generate the nonlinear improvement of the linear witness $W_L^{\Psi^+}$, but in this case we require $U = \sigma_z \otimes \sigma_z$ to achieve the same result. The general form of the nonlinear witness and the measurements required to implement it are shown in the Supplemental Material [30].

Experiment results.—Before we calculate the entanglement witnesses, we perform quantum state tomography on each input state. We find that our method of quantum state preparation is able to produce a wide range of quantum states of the form given in Eqs. (2) and (3) to a high degree of confidence. In particular, Fig. 2 shows reconstructed states very close to the maximally entangled Bell states in the orbital angular momentum degree of freedom. We find fidelities of 97% between each anticorrelated state and the corresponding $|\Psi^\pm\rangle$ Bell state and 85% between each correlated state and the corresponding $|\Phi^\pm\rangle$ Bell state.

We note that in our case, because of the differing OAM values that we detect, our states are not maximally entangled, but it would be simple to extract out the maximally entangled Bell states if necessary. These states are obtained when the $|0, 0\rangle$ term in Eq. (2) [or Eq. (3)] is replaced by a $|-\ell, -\ell\rangle$ term (or a $|\ell, -\ell\rangle$ term). In other words, the absolute values of all of the OAM states of

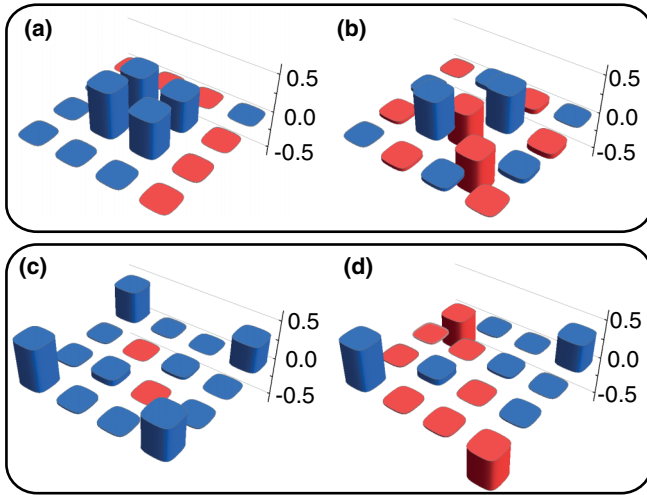


FIG. 2 (color online). Real parts of the density matrices of anticorrelated states with phase $\phi = 0$ (a) and $\phi = \pi$ (b) between the modes and correlated states with phase $\phi = 0$ (c) and $\phi = \pi$ (d) between the modes. These are extremely close to the maximally entangled Bell states, with differences occurring due to the relative coefficients of the OAM values $\ell = 0$ and $\ell = \pm 2$ that we choose to detect. The anticorrelated states both have fidelity 97% with their respective maximally entangled Bell states $|\Psi^\pm\rangle$, and the correlated states both have fidelity 85% with their respective maximally entangled states $|\Phi^\pm\rangle$. The average of the absolute values of the imaginary parts is 0.01 ± 0.01 .

interest are the same. For example, to measure an anticorrelated Bell state for $|\ell| = 2$, the measurements would be restricted to the subspaces with the OAM values $|2, -2\rangle$ and $|-2, 2\rangle$. However, in accordance with Eqs. (2) and (3), we measure modes $\ell = 0$ and $\ell = \pm 2$ such that the coefficients are slightly different, and thus we reconstruct states very close to the maximally entangled states.

In Fig. 3, we see that a single nonlinear witness is able to verify the entanglement of a large range of input states, that is, states of the form either ρ^Φ or ρ^Ψ . In contrast, no single linear witness is able to verify entanglement over the same range; the expectation value of each linear witness is above zero for half of the states we measure. Since we use quantum state tomography to confirm that our states are entangled, this means that each linear witness delivers an inconclusive result and thus cannot detect entanglement in a large range of states that are entangled. These results are for the two-dimensional subspaces described in Eqs. (2) and (3) where $\ell = 2$.

In the anticorrelated case, all expectation values of the nonlinear witness are negative, indicating entangled states for all phases observed. In the correlated case, the nonlinear witness is negative for the majority of the observed states. However, near $\pi/2$ and $3\pi/2$, there are three states that have slightly positive expectation values.

Discussion.—Our results show that a wide range of two-photon entangled states can be prepared by using a combination of parametric down-conversion and suitably oriented Dove prisms. The nonlinear witness expectation values clearly show that we can establish the entanglement of the relevant classes of states. In particular, this method produces the entangled Bell states $|\Psi^\pm\rangle$ and $|\Phi^\pm\rangle$.

We note that the correlated states have a lower fidelity than the anticorrelated states when compared with the maximally entangled Bell states. We attribute this reduction in fidelity to the asymmetry introduced when only one Dove prism is present. This discrepancy between the correlated and anticorrelated OAM states also highlights an interesting aspect of nonlinear entanglement witnesses: the extreme sensitivity of the expectation value with regards to the outcome of a single projective measurement. As can be seen from Eq. (5), the last term that is subtracted in the calculation is inversely proportional to $1 - |\text{Tr}[\rho(-\sigma_z \otimes \sigma_z)]|^2$ (one minus the square of the contrast of the OAM correlations), and, consequently, the precise expectation value that is measured is highly sensitive to $\text{Tr}[\rho(-\sigma_z \otimes \sigma_z)]$. As the strength of the OAM correlations depends critically on a few measurements, so too does the obtained value of w_∞ .

The difference in the range of measured expectation values originates in the strength of the OAM correlations for each case. For the anticorrelated states of the form ρ^Ψ , the average measured value of $|\text{Tr}[\rho(-\sigma_z \otimes \sigma_z)]|$ was equal to 0.92, whereas for the correlated states of the form ρ^Φ , the average measured value of $|\text{Tr}[\rho(-\sigma_z \otimes \sigma_z)]|$ was

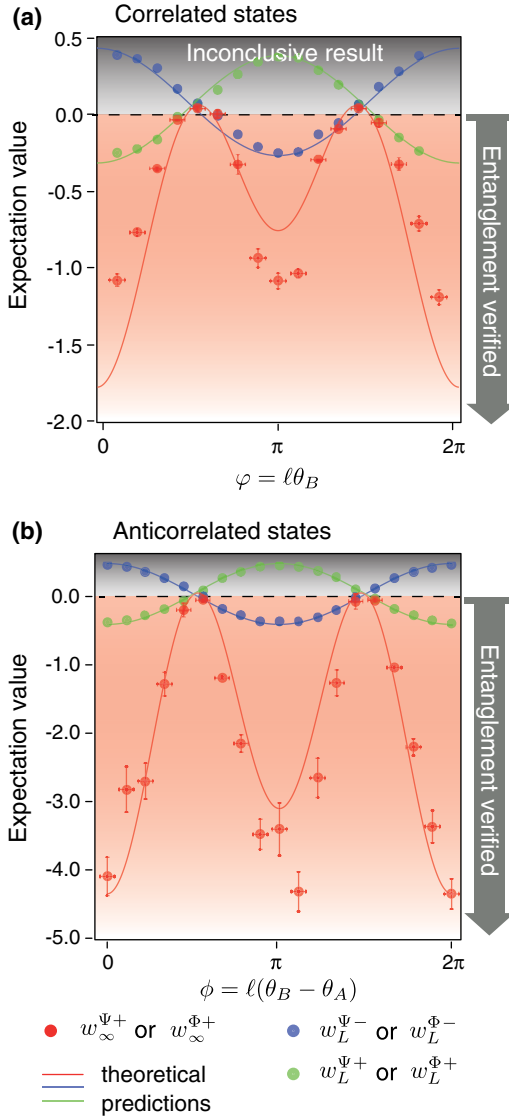


FIG. 3 (color online). Experimentally recorded expectation values of the nonlinear entanglement witness and the two linear witnesses for correlated (a) and anticorrelated (b) entangled states for $\ell = 2$. A negative expectation value indicates that the state is entangled. Note that the nonlinear witness correctly detects entanglement under almost all cases, whereas each of the linear witnesses often fails to detect entanglement, even though it is present. For the correlated states, we measured $w_\infty^{\Psi^+}$, $w_L^{\Phi^+}$, and $w_L^{\Phi^-}$, and for the anticorrelated states, we measured $w_\infty^{\Psi^+}$, $w_L^{\Psi^+}$, and $w_L^{\Psi^-}$. The circles give the experimental data points, and the lines are theoretical predictions obtained by using average parameters obtained from the data. The vertical error bars were obtained by applying \sqrt{N} fluctuations to the measured coincidence counts and then averaging over 100 iterations to obtain the standard deviation. The horizontal error bars are estimated to be $\pi/24$.

equal to 0.69. The theoretical fits to the data are adjusted to reflect the appropriate measured contrasts.

In certain situations it would be desirable to further increase the range of states accessible to nonlinear

witnesses. There are two possible avenues for doing so. The first method involves adjusting the exact form of the witness. The only degree of flexibility in the construction of the accessible nonlinear witnesses described in Ref. [27] is in the choice of unitary operator U . For our particular choice of U , a nonlinear improvement on a correlated linear witness will not be able to detect entanglement in anticorrelated states, and vice versa. Other choices of U are possible, for example, $U = (\mathbb{1} - \sigma_x \otimes \sigma_x - \sigma_y \otimes \sigma_y + \sigma_z \otimes \sigma_z)/2$; in this case, $U = 2W_L^{\Psi^+}$. With this choice of U , the nonlinear witness can access different states. More specifically, starting with a linear witness ($W_L^{\Psi^+}$) that detects anticorrelated states, the nonlinear improvement using $U = 2W_L^{\Psi^+}$ can detect both anticorrelated and correlated states.

The second method involves using two carefully chosen nonlinear witnesses. In fact, by using two nonlinear witnesses, it is possible to extend the range sufficiently to detect entanglement in all qubit entangled states. For example, this can be achieved by using the two witnesses shown in this Letter: one witness that detects the correlated states (e.g., $W_\infty^{\Phi^+}$) and one witness that detects the anticorrelated states (e.g., $W_\infty^{\Psi^+}$). Using these two witnesses enables the verification of entanglement of the full range of pure quantum states, which includes all four Bell states, with only ten measurements.

Conclusions.—The orbital angular momentum of light is increasingly becoming an important resource for quantum information science. Consequently, it is important to develop a universal set of gates for the spatial degree of freedom that can then be used for quantum information processing. The laboratory procedures that we have developed are important for the generation and controlled manipulation of many different entangled quantum states. These operations have particular relevance in applications such as superdense coding and quantum teleportation. As entanglement is a fundamental tool in many quantum information applications, the efficient detection of entangled states is paramount to the use of such quantum technologies. We have demonstrated the use of accessible nonlinear witnesses to verify entanglement in twice as many states as a single linear witness can. This enhanced detection range requires no more measurements than are required for the linear witness. We envisage the continued application of nonlinear witnesses to other areas of quantum information science, where it is advantageous to extract maximal information with the minimum number of measurements.

We thank J.M. Arrazola, O. Gittsovich, and N. Lütkenhaus for valuable discussions regarding this work. This work was supported by the Canada Excellence Research Chairs (CERC) Program and the Natural Sciences and Engineering Research Council of Canada (NSERC). R.W.B. thanks the DARPA InPho program for financial support.

- [1] M. D. Reid, P. D. Drummond, W. P. Bowen, E. G. Cavalcanti, P. K. Lam, H. A. Bachor, U. L. Andersen, and G. Leuchs, *Rev. Mod. Phys.* **81**, 1727 (2009).
- [2] C. H. Bennett and S. J. Wiesner, *Phys. Rev. Lett.* **69**, 2881 (1992).
- [3] J. Barreiro, T. Wei, and P. Kwiat, *Nat. Phys.* **4**, 282 (2008).
- [4] A. Mair, A. Vaziri, G. Weihs, and A. Zeilinger, *Nature (London)* **412**, 313 (2001).
- [5] E. Nagali, L. Sansoni, F. Sciarrino, F. De Martini, L. Marrucci, B. Piccirillo, E. Karimi, and E. Santamato, *Nat. Photonics* **3**, 720 (2009).
- [6] E. Nagali, F. Sciarrino, F. De Martini, L. Marrucci, B. Piccirillo, E. Karimi, and E. Santamato, *Phys. Rev. Lett.* **103**, 013601 (2009).
- [7] J. Leach, B. Jack, J. Romero, A. Jha, A. Yao, S. Franke-Arnold, D. Ireland, R. Boyd, S. Barnett, and M. Padgett, *Science* **329**, 662 (2010).
- [8] R. Fickler, R. Lapkiewicz, W. N. Plick, M. Krenn, C. Schaeff, S. Ramelow, and A. Zeilinger, *Science* **338**, 640 (2012).
- [9] X. Cai, J. Wang, M. J. Strain, B. Johnson-Morris, J. Zhu, M. Sorel, J. L. O'Brien, M. G. Thompson, and S. Yu, *Science* **338**, 363 (2012).
- [10] O. Gühne and G. Tóth, *Phys. Rep.* **474**, 1 (2009).
- [11] M. Lewenstein, B. Kraus, J. I. Cirac, and P. Horodecki, *Phys. Rev. A* **62**, 052310 (2000).
- [12] D. Bruß, *J. Math. Phys. (N.Y.)* **43**, 4237 (2002).
- [13] O. Gühne, P. Hyllus, D. Bruß, A. Ekert, M. Lewenstein, C. Macchiavello, and A. Sanpera, *Phys. Rev. A* **66**, 062305 (2002).
- [14] G. M. D'Ariano, C. Macchiavello, and M. G. A. Paris, *Phys. Rev. A* **67**, 042310 (2003).
- [15] A. O. Pittenger and M. H. Rubin, *Phys. Rev. A* **67**, 012327 (2003).
- [16] R. A. Bertlmann, K. Durstberger, B. C. Hiesmayr, and P. Krammer, *Phys. Rev. A* **72**, 052331 (2005).
- [17] M. Barbieri, F. De Martini, G. Di Nepi, P. Mataloni, G. M. D'Ariano, and C. Macchiavello, *Phys. Rev. Lett.* **91**, 227901 (2003).
- [18] M. Bourennane, M. Eibl, C. Kurtsiefer, S. Gaertner, H. Weinfurter, O. Gühne, P. Hyllus, D. Bruß, M. Lewenstein, and A. Sanpera, *Phys. Rev. Lett.* **92**, 087902 (2004).
- [19] M. Agnew, J. Leach, and R. W. Boyd, *Eur. Phys. J. D* **66**, 6 (2012).
- [20] J. Uffink, *Phys. Rev. Lett.* **88**, 230406 (2002).
- [21] V. Giovannetti, S. Mancini, D. Vitali, and P. Tombesi, *Phys. Rev. A* **67**, 022320 (2003).
- [22] J. B. Altepeter, E. R. Jeffrey, P. G. Kwiat, S. Tanzilli, N. Gisin, and A. Acin, *Phys. Rev. Lett.* **95**, 033601 (2005).
- [23] F. A. Bovino, G. Castagnoli, A. Ekert, P. Horodecki, C. M. Alves, and A. V. Sergienko, *Phys. Rev. Lett.* **95**, 240407 (2005).
- [24] P. Hyllus and J. Eisert, *New J. Phys.* **8**, 51 (2006).
- [25] O. Gühne and N. Lütkenhaus, *Phys. Rev. Lett.* **96**, 170502 (2006).
- [26] Z.-W. Wang, Y.-F. Huang, X.-F. Ren, Y.-S. Zhang, and G.-C. Guo, *Europhys. Lett.* **78**, 40002 (2007).
- [27] J. M. Arrazola, O. Gittsovich, and N. Lütkenhaus, *Phys. Rev. A* **85**, 062327 (2012).
- [28] M. Agnew, J. Leach, M. McLaren, F. S. Roux, and R. W. Boyd, *Phys. Rev. A* **84**, 062101 (2011).
- [29] T. Moroder, O. Gühne, and N. Lütkenhaus, *Phys. Rev. A* **78**, 032326 (2008).
- [30] See Supplemental Material at <http://link.aps.org/supplemental/10.1103/PhysRevLett.111.030402> for further details of the experimental setup and the general form and measurements of the nonlinear witness.